

Coordination chemistry of flexible benzene-1,3,5-tricarboxamide derived carboxylates; notable structural resilience and vaguely familiar packing motifs

Amy D. Lynes,^{a*} Chris S. Hawes,^{a,b} Kevin Byrne,^c Wolfgang Schmitt,^c and Thorfinnur Gunnlaugsson^{a*}

^aSchool of Chemistry and Trinity Biomedical Sciences Institute (TBSI), The University of Dublin, Trinity College Dublin, Dublin 2, Ireland. gunnlaut@tcd.ie; lynesa@tcd.ie

^bSchool of Chemical and Physical Sciences, Keele University, Keele, ST5 5BG, United Kingdom

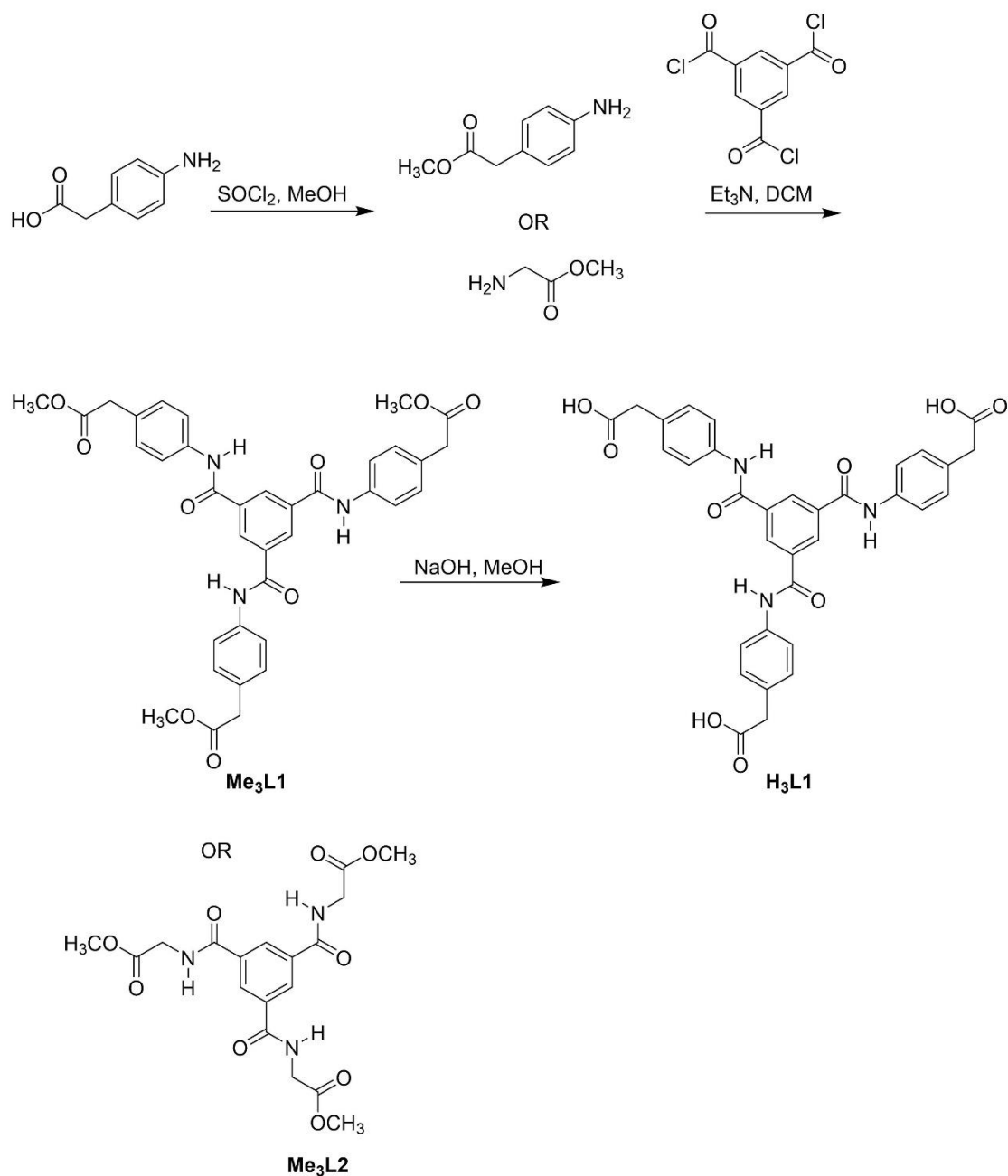
^cSchool of Chemistry, Centre for Research on Adaptive Nanostructures and Nanodevices (CRANN), The University of Dublin, Trinity College Dublin, Dublin 2, Ireland

Supporting Information

Synthesis	2
X-Ray powder diffraction	4
NMR Spectra	6
Thermogravimetric analysis	10
Infrared spectroscopy	11
X-ray Crystallography	13
Gas Adsorption Data	15
References	18

1. Synthesis

1.1. General synthetic scheme



1.2 Synthetic procedures

Synthesis of methyl 2-(4-aminophenyl)acetate

4-Aminophenylacetic acid (3 g, 19.8 mmol) was dissolved in 100 mL of CH_3OH , then cooled in ice before the dropwise addition of SOCl_2 (7.06 g, 4.2 mL, 59.4 mmol). Solution was left to stir for 12 hr at room temperature. SOCl_2 and CH_3OH were then removed by vacuum distillation to yield a yellow solid which was dried *in vacuo* (3.3 g, 19.5 mmol, 98 %); mp (decomp) > 185 °C. δ_{H} ($\text{DMSO}-d_6$, 600 MHz) 7.35 (d, $J = 8.3$ Hz, 2H, Aromatic), 7.28 (d, $J =$

8.2 Hz, 2H, Aromatic), 3.71 (s, 2H, CH₂), 3.61 (s, 3H, CH₃; δ_C (DMSO-*d*₆, 150 Hz) 171.4 (RCOOCH₃), 133.6 (Aromatic), 130.7 (Aromatic), 122.5 (Aromatic), 51.8 (CH₃), 39.6 (CH₂, overlapping DMSO); *m/z* (HRMS-ESI⁺): [M+H]⁺ calcd for C₉H₁₁NO₂, 166.0868, found 166.0869; ν_{\max} (cm⁻¹): 2769, 2584, 1772, 1614, 1565, 1515, 1436, 1357, 1218, 1172, 995, 950, 901, 810, 772, 719, 684.

Synthesis of trimethyl 4, 4', 4''-((1,3,5-benzenetriyltris(carboxamide)-tris-phenylacetate) Me₃L1

Methyl 2-(4-aminophenyl)acetate (0.3 g, 1.7 mmol) was dissolved in dry DCM (20 mL), then cooled in ice before the addition of Et₃N (0.34 g, 0.45 mL, 2.5 mmol). 1, 3, 5-Benzenetricarbonyl trichloride was dissolved in dry DCM (10 mL) and added to the solution of methyl 2-(4-aminophenyl)acetate and Et₃N, with the resulting mixture stirred under argon at room temperature for 24 hr. The solution was washed with NaHCO₃ solution in H₂O three times, with the organic layer collected and evaporated to reveal a yellow solid. To purify, the solid was dissolved in 40 mL KOH solution (1 M) and 40 mL DCM and stirred at room temperature for 3 hr. The organic layer was then then separated and washed with water, with the DCM then evaporated to reveal a pale yellow solid (0.15 g, 0.23 mmol, 45 %); mp 188-197 °C; δ_H (DMSO-*d*₆, 600 MHz) 10.58 (s, 3H, NH), 8.69 (s, 3H, 1), 7.76 (d, *J* = 8.4 Hz, 6H, Aromatic), 7.29 (d, *J* = 8.4 Hz, 6H, Aromatic), 3.67 (s, 6H, CH₂), 3.63 (s, 9H, CH₃); δ_C (DMSO-*d*₆, 150 Hz) 171.7 (RCOOCH₃), 165.5 (RCONH), 137.7 (Aromatic), 135.5 (Aromatic), 129.9 (C1), 129.6 (Aromatic), 120.4 (Aromatic), 51.2 (CH₃) 39.6 (CH₂ overlapping DMSO); *m/z* (HRMS-ESI⁺) [M+Na]⁺ calcd for C₃₆H₃₃N₃O₉Na, 674.2106, found 674.2114; ν_{\max} (cm⁻¹): 3348, 2942, 2853, 1729, 1643, 1601, 1514, 1434, 1411, 1315, 1255, 1196, 1152, 1093, 1011, 917, 846, 797, 698.

2. X-ray Powder Diffraction

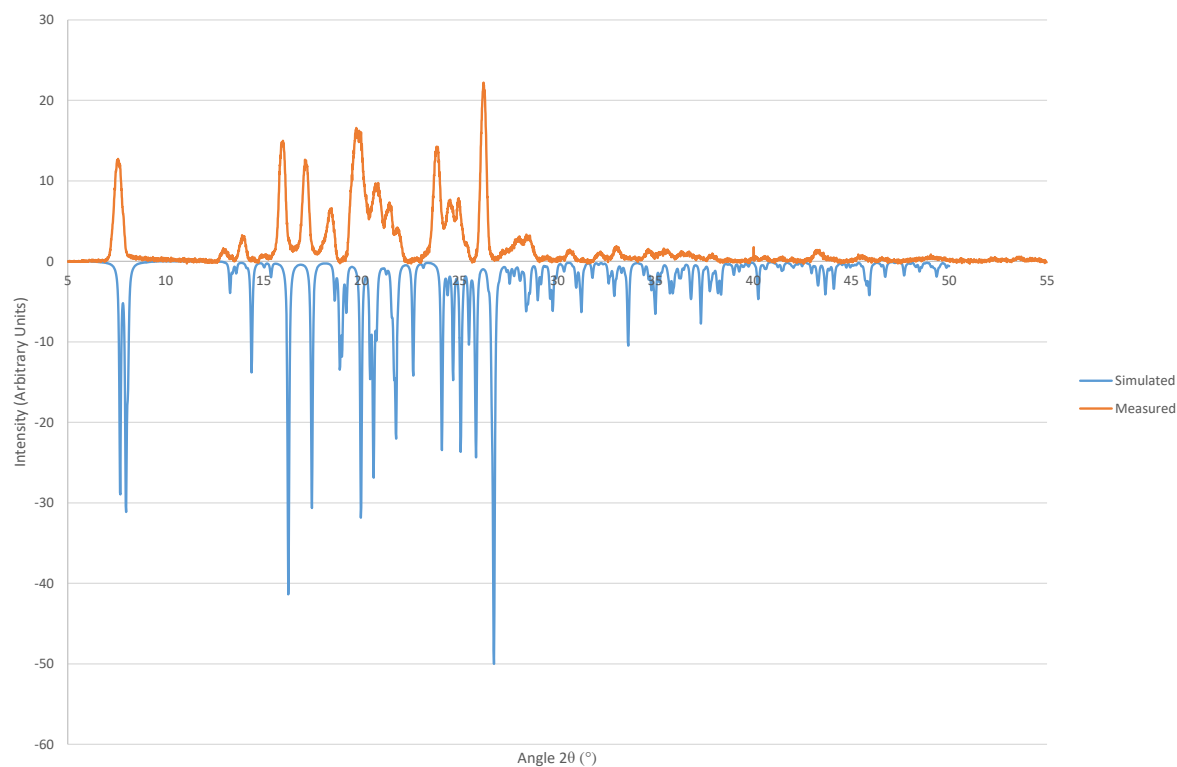


Figure S1 X-ray powder diffraction pattern for compound **Me₃L2**, measured at room temperature and compared to the simulated pattern from the single-crystal data collected at 100K.

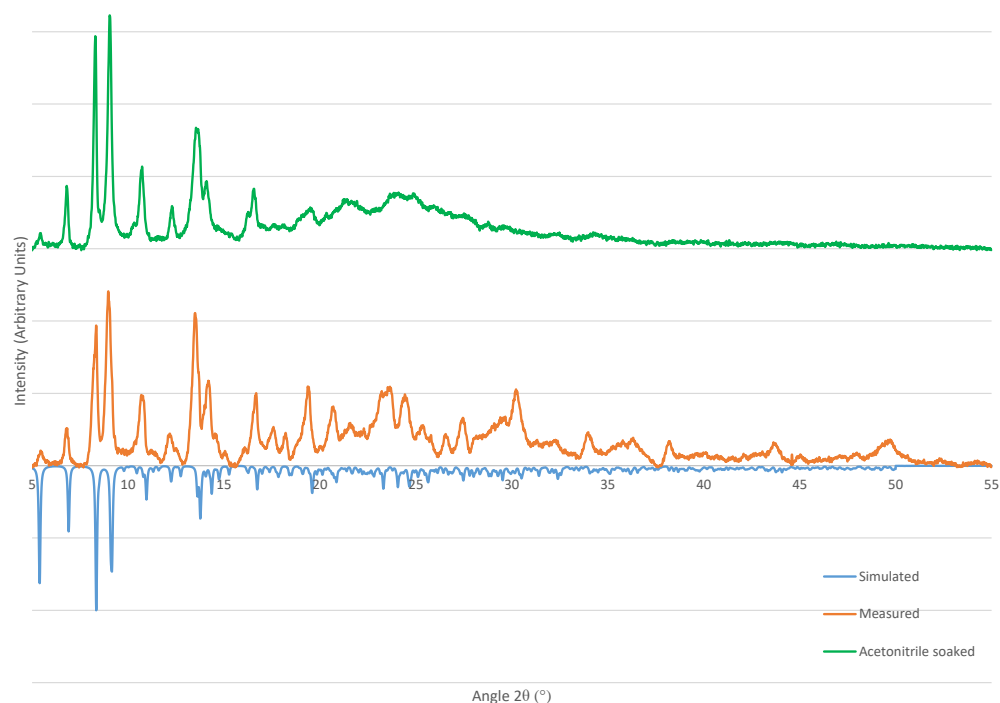


Figure S2 X-ray powder diffraction pattern for complex **1** at room temperature, and the pattern obtained for the acetonitrile-soaked material following the gas adsorption experiment, compared to the simulated pattern from the single-crystal data collected at 100K.

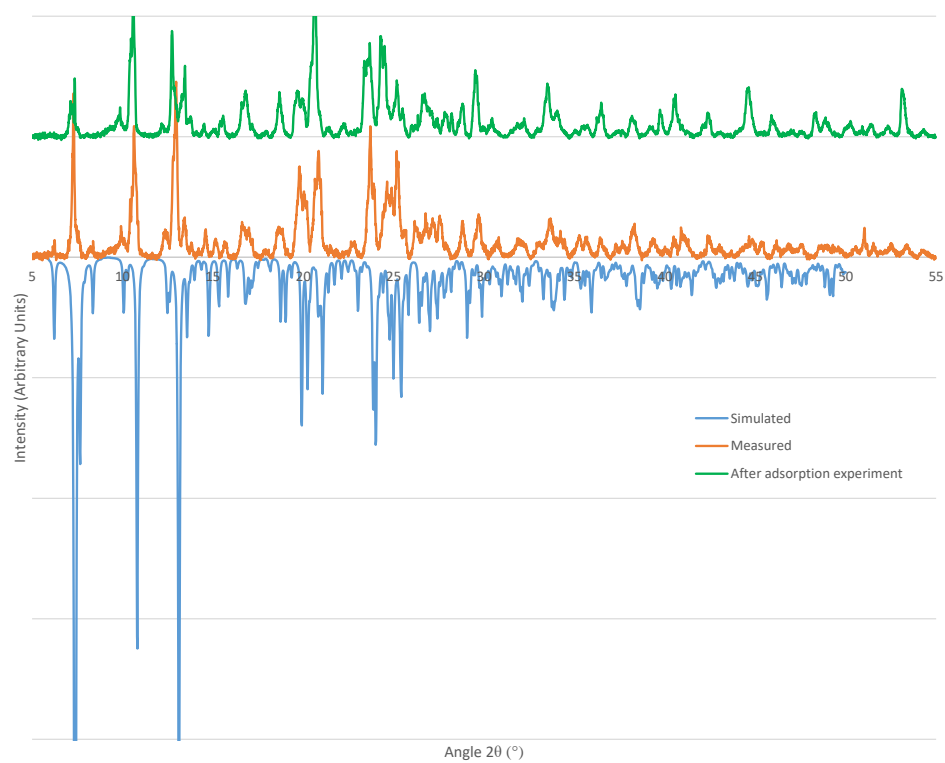


Figure S3 X-ray powder diffraction pattern for complex **2**, measured at room temperature and measured after the adsorption experiment compared to the simulated pattern from the single-crystal data collected at 100K.

3. NMR Spectra

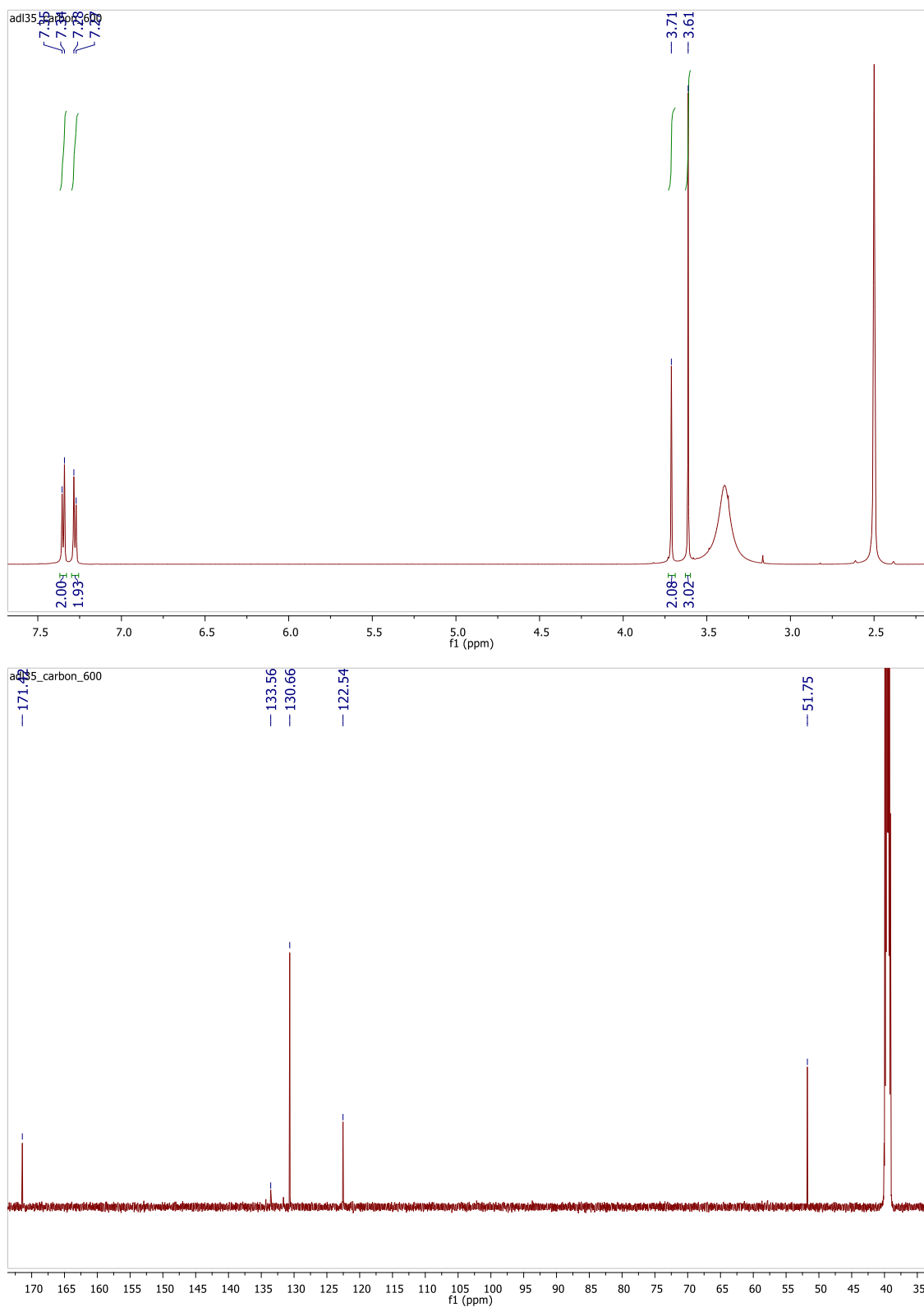


Figure S4 ¹H NMR and ¹³C NMR of methyl 4-aminophenylacetate

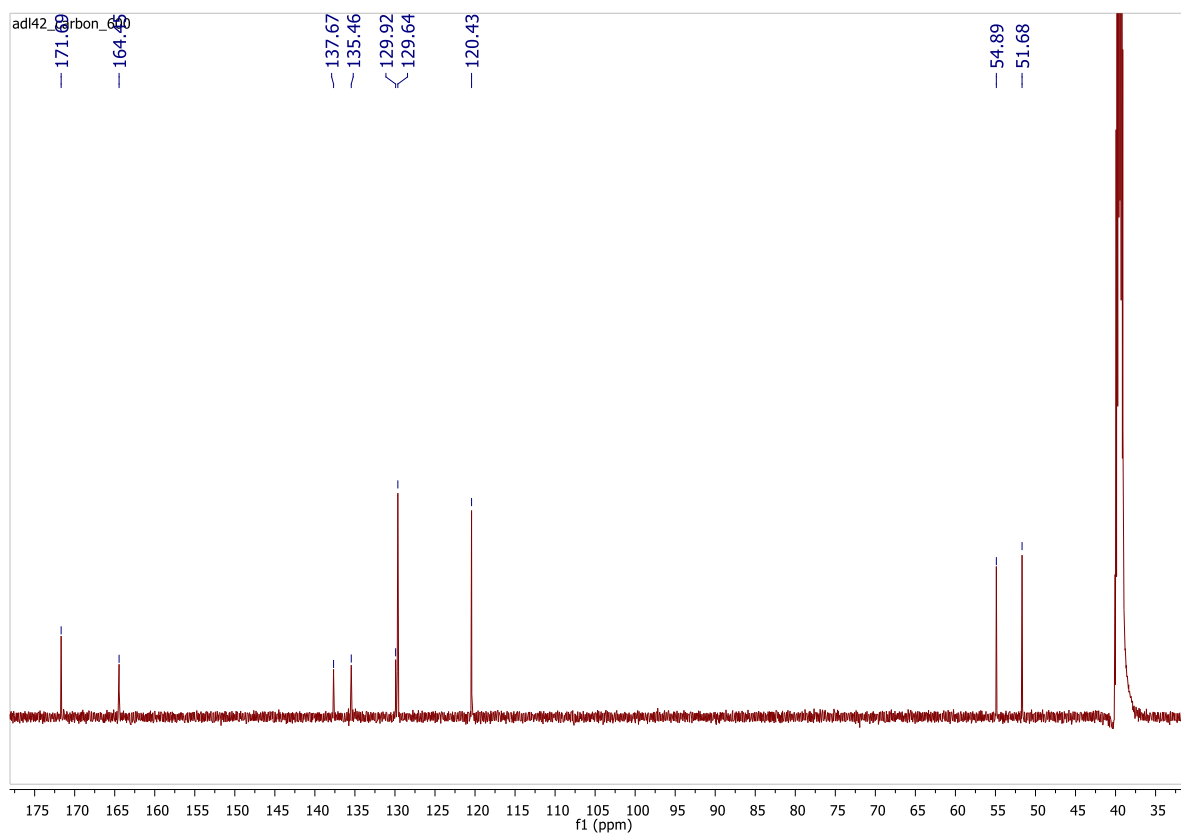
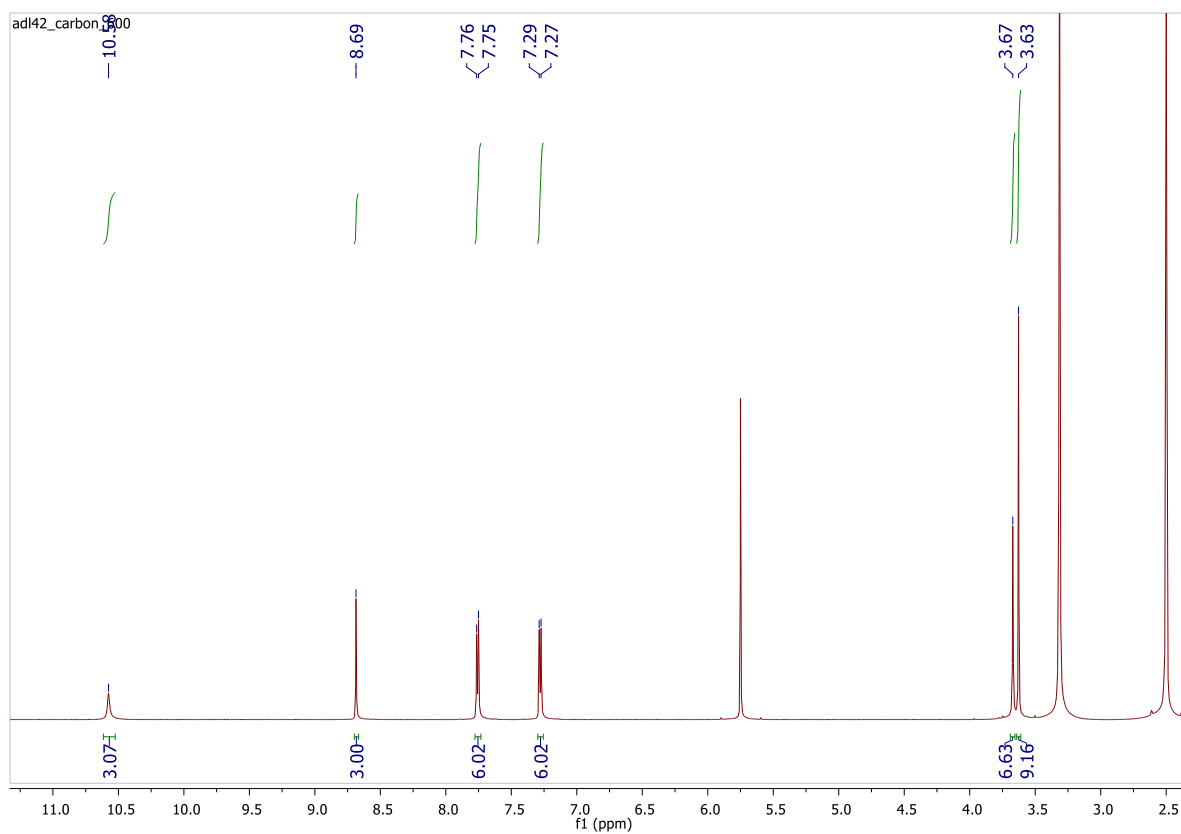


Figure S5 ^1H NMR and ^{13}C NMR of $\text{Me}_3\text{L1}$

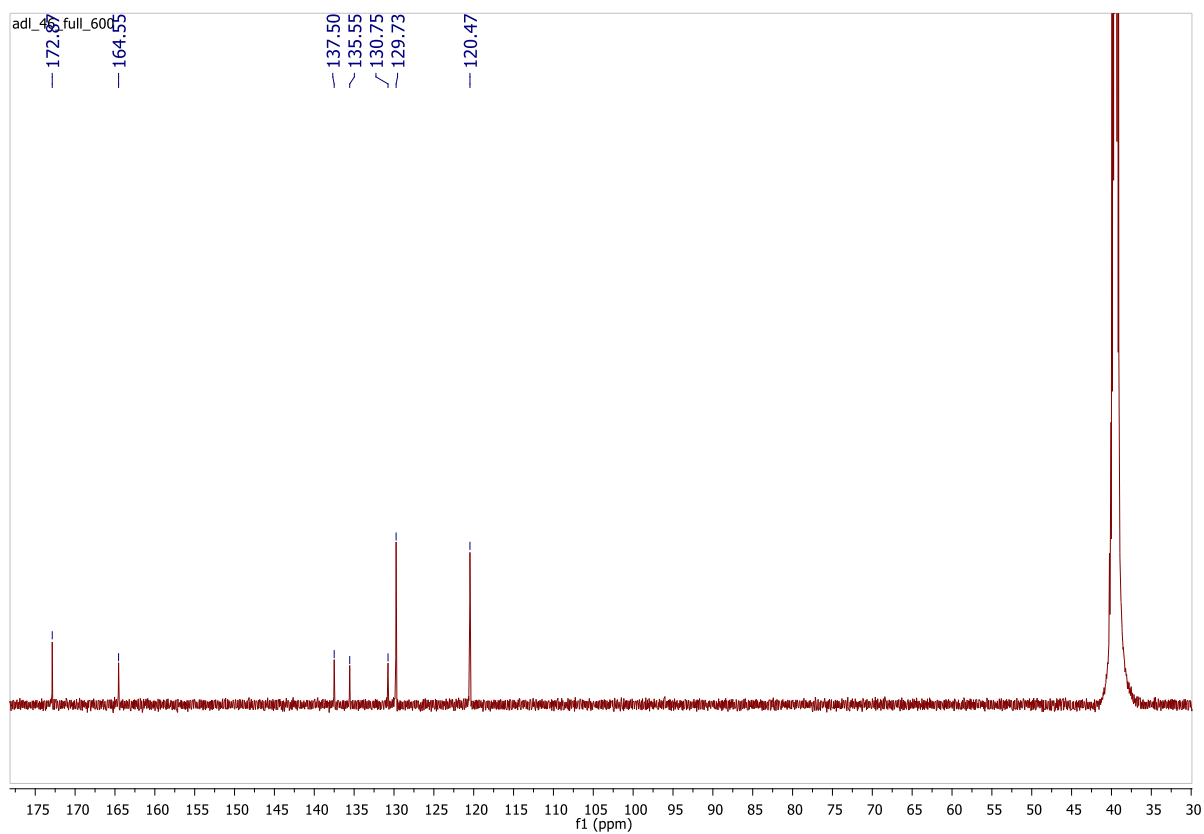
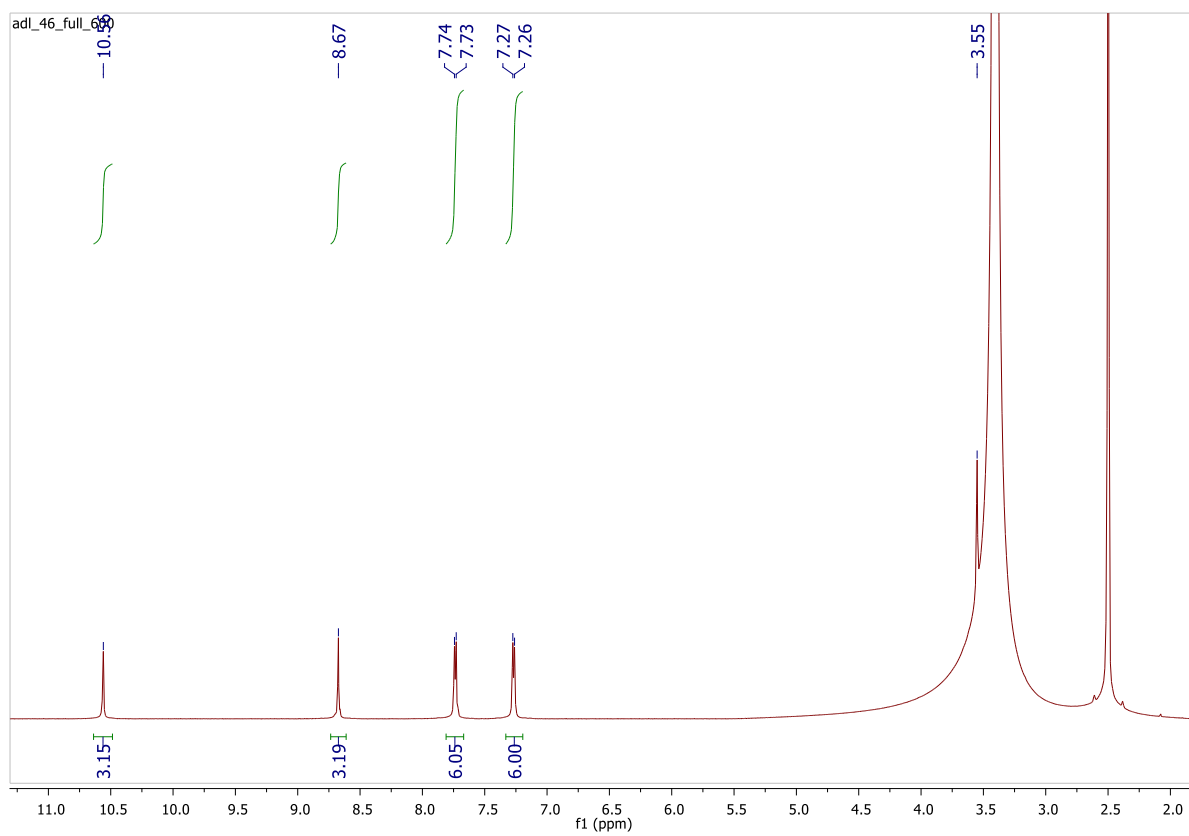


Figure S6 ^1H NMR and ^{13}C NMR of $\text{H}_3\text{L1}$

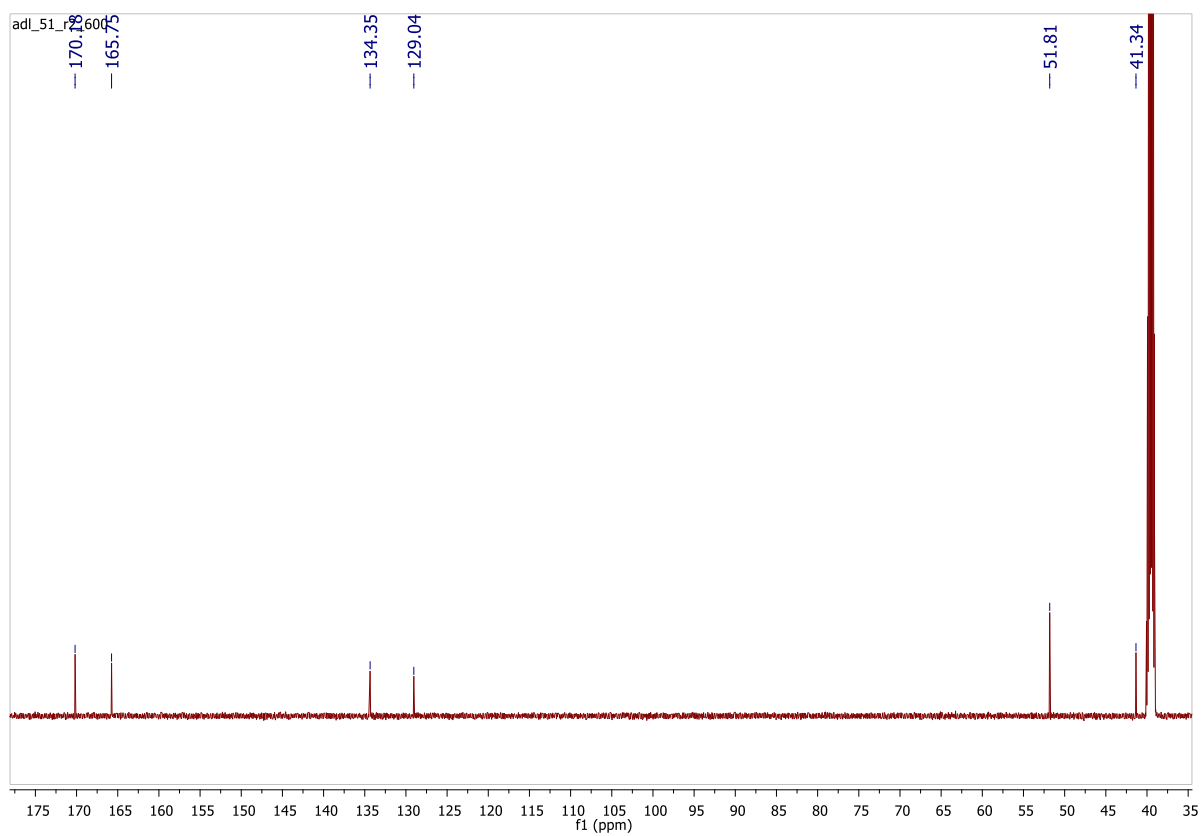
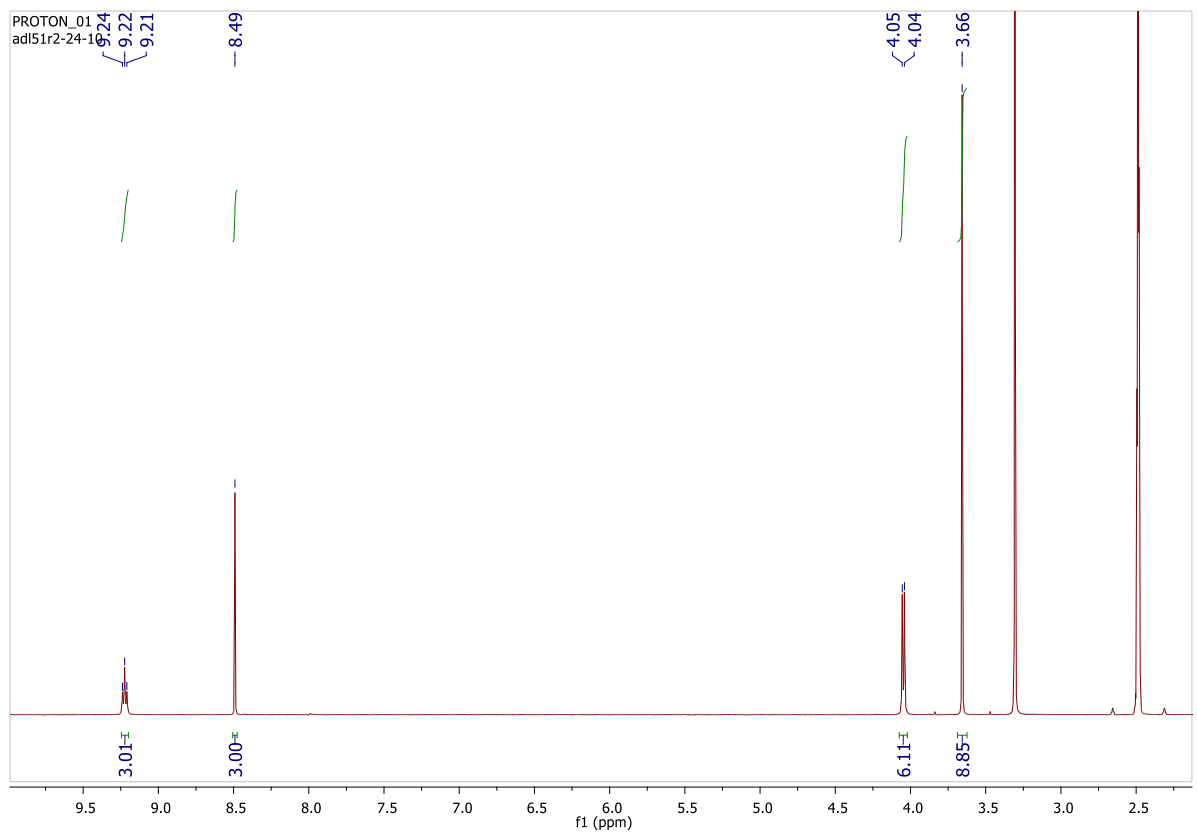


Figure S7 ^1H NMR and ^{13}C NMR of $\text{Me}_3\text{L2}$

4. Thermogravimetric analysis

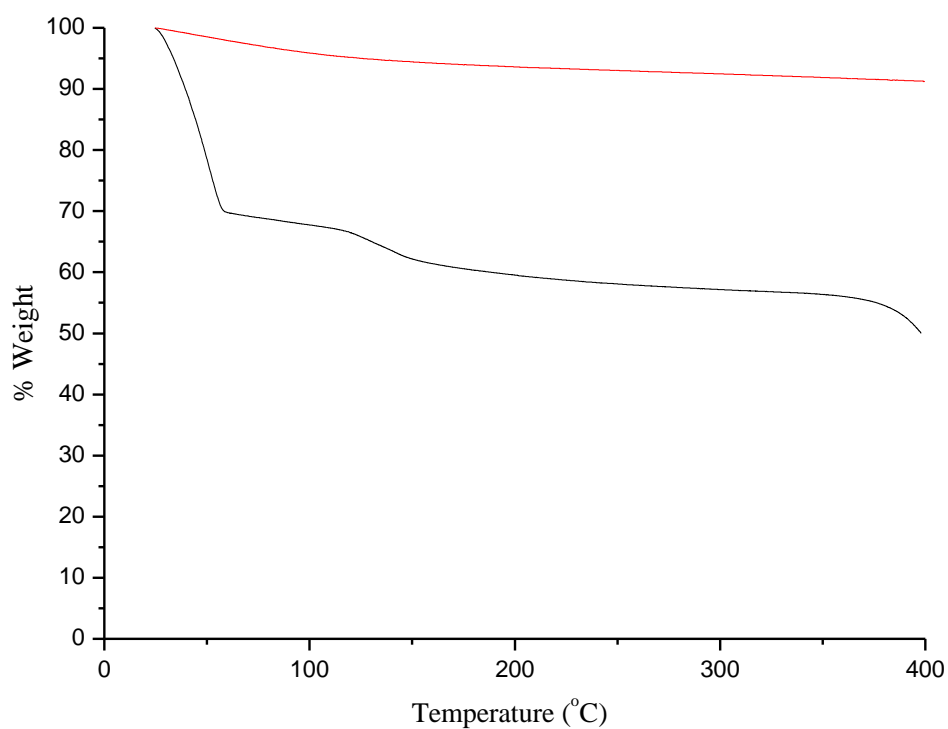


Figure S8 Thermogravimetric analysis trace for complex **1** freshly isolated (black) and following MeCN exchange (red).

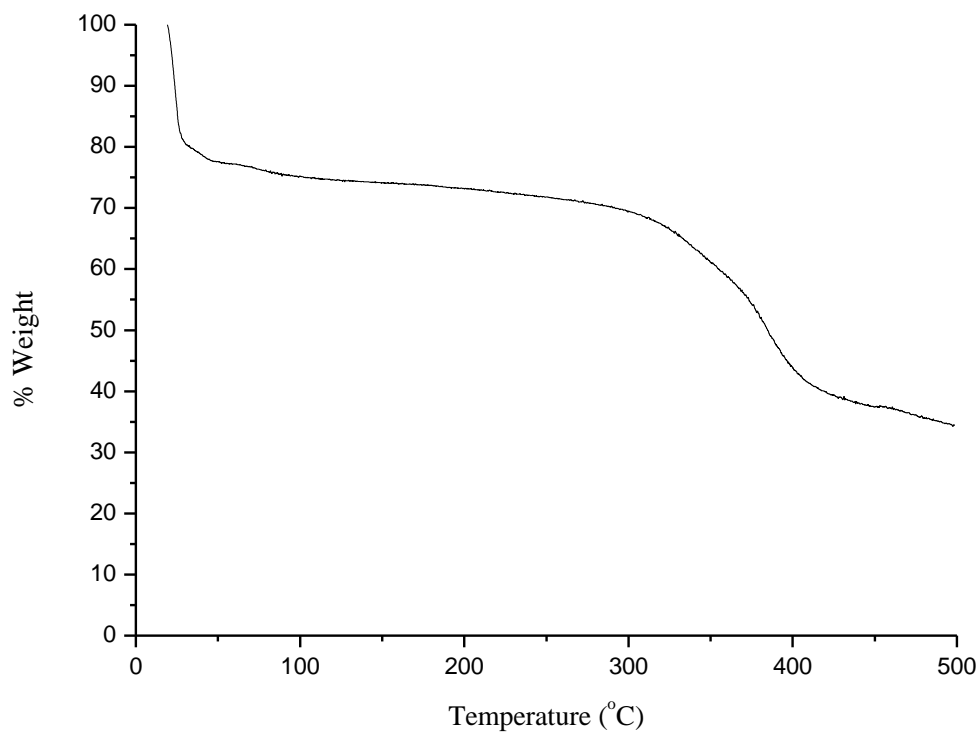


Figure S9 Thermogravimetric analysis trace for complex **2**

5. Infrared spectroscopy

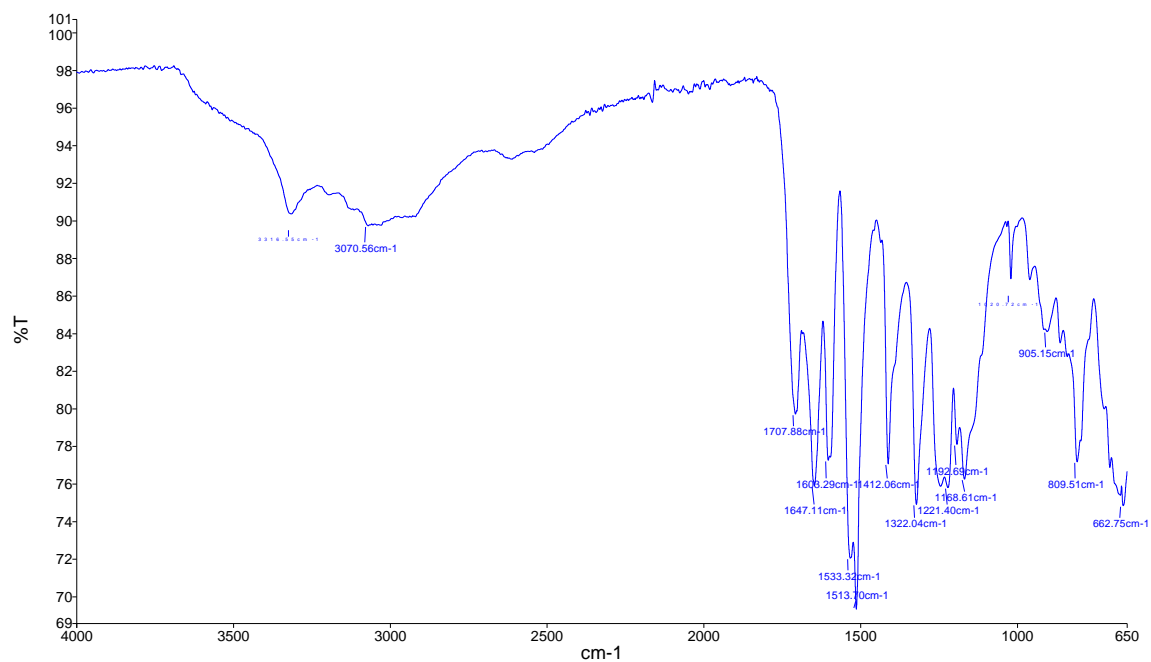


Figure S10 IR spectrum of H₃L₂

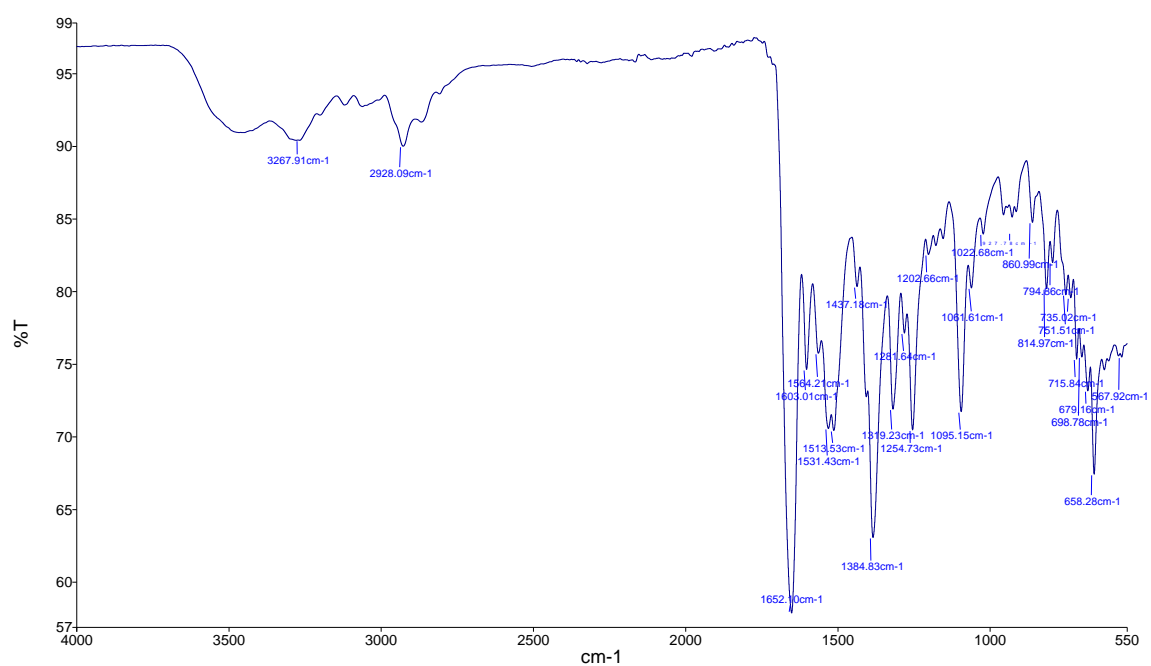


Figure S11 IR spectrum of complex 1

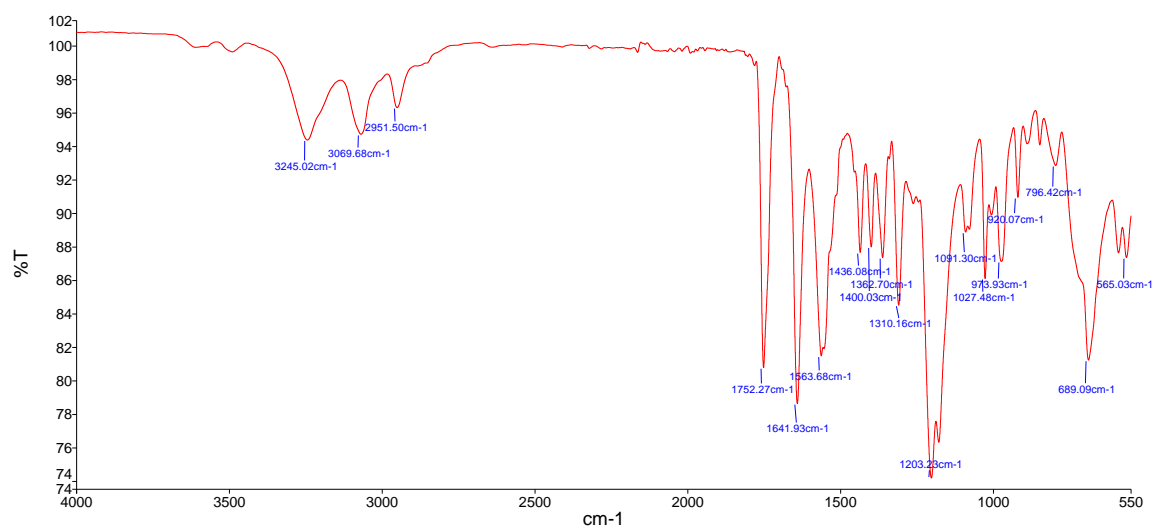


Figure S12 IR spectrum of Me₃L₂

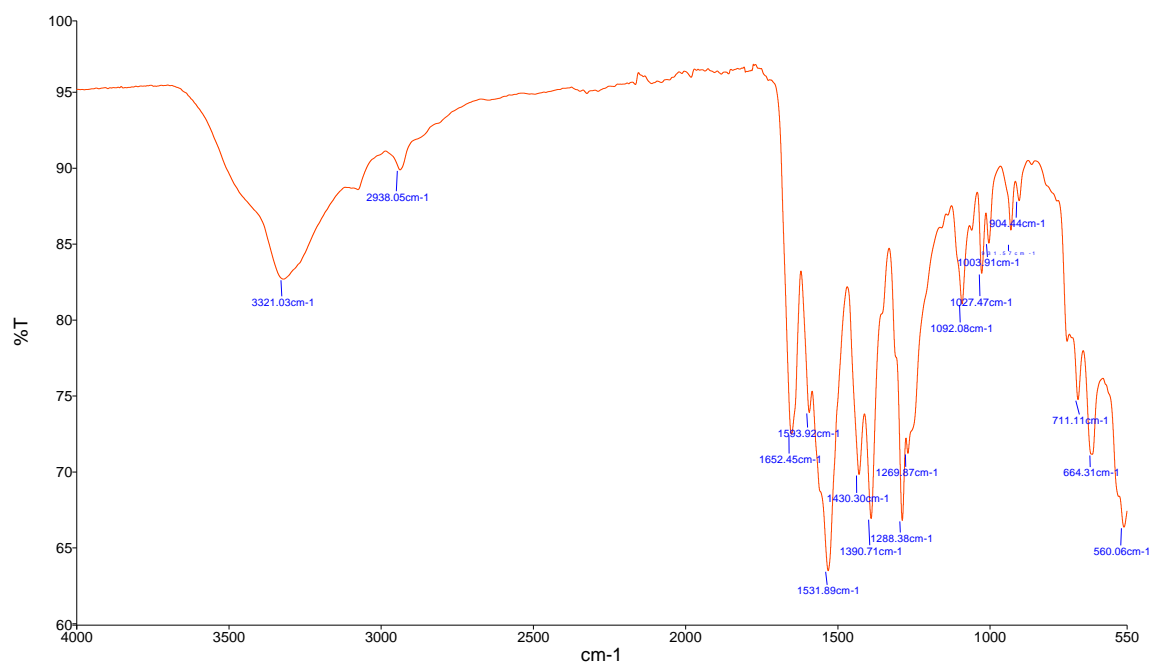


Figure S13 IR spectrum of complex 2

6. X-ray Crystallography

For the structures of **Me₃L2** and complex **2**, only minor disorder in one ester group or two lattice water molecules, respectively, were evident, and these were modelled at partial occupancies with PART cards and distance / U_{ij} restraints where necessary to maintain reasonable geometries and hydrogen bonding behaviour. In the case of complex **1**, modelling the complete structure from the initial solution gave the complete connectivity model but two prominent Fourier residuals were evident in the vicinity of Cd2 and Cd3 at 9.68 and 12.42 $e \cdot \text{\AA}^{-3}$. Absorption or truncation artifacts were discounted by the invariance of these residuals to heavier absorption corrections or reducing the data resolution, as well as the lack of symmetry for the major residuals about the heavy atoms. Modelling both residuals as Cd sites with free occupancies tied to the nearest Cd atom, both sites refined to occupancies of approximately 15%, which were subsequently fixed, with Cd2 and Cd3 fixed at 0.85 occupancy. This led to an immediate improvement in refinement parameters; the best available R_1 (all data) was 0.1320 ($R_{1(I>2\sigma(I))} = 0.0935$) prior to modelling the additional cadmium sites, while the final parameters were R_1 (all data) = 0.0876 and $R_{1(I>2\sigma(I))} = 0.0496$. This is also represented in Figure S10 below. A small amount of residual electron density was also located nearby to Cd1; modelling this as a further disordered contributor did not improve the refinement by an amount sufficient to justify the additional restraints and parameters necessary.

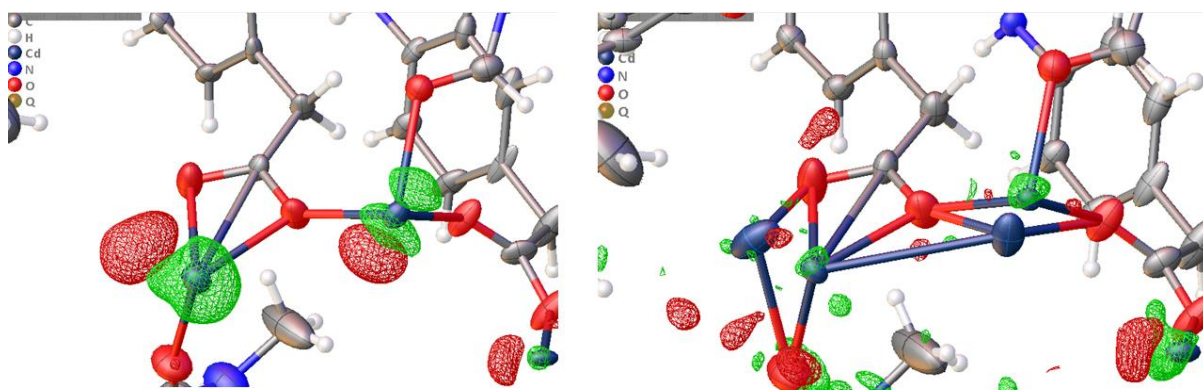


Figure S14 Residual electron density maps for complex **1** before (left, rendered at $\pm 1.4 e \cdot \text{\AA}^{-3}$) and after (right, rendered at $\pm 0.9 e \cdot \text{\AA}^{-3}$) modelling the disorder around cadmium sites Cd2 and Cd3.

Following this, carboxylate groups which exhibited nonsensical bond lengths to the minor component atoms (Cd2A and Cd3A) were split and modelled in chemically reasonable positions although, due to the low occupancy of the minor component and proximity to several heavy atoms, these were heavily restrained with DFIX, SADI and ISOR restraints. Where sensible U_{ij} parameters could not be achieved, the ADPs of the minor component atoms (labelled with suffix A) were constrained with EADP to the nearby equivalent atom from the major contributor. Bond distances and angles for the major contributor were mostly allowed to freely refine, but those for the minor contributor are largely fixed and not necessarily representative of the true distances. Furthermore, the non-carboxylate (i.e. DMF or aqua) ligands completing the coordination spheres of Cd2A and Cd3A could not be located from Fourier residuals; rather than arbitrarily adding these groups to the model, we have retained the model with only the groups which could be reasonably located from the diffraction data, with the rationale that (as is the case in many porous systems) the true formulation was better described by supporting bulk-phase methods. In addition, hydrogen atoms for the partial-occupancy O25 water site could not be located or modelled reasonably; these were however added to the crystallographic formula to best represent the chemical species present within the model.

Table S1 Crystal and refinement parameters for all data collections

Identification code	Me₃L2	1	2
Empirical formula	C ₁₈ H ₂₂ N ₃ O _{9.5}	C _{79.05} H _{81.45} Cd ₃ N _{10.35} O _{24.7}	C ₃₃ H ₄₇ Cd ₃ N ₇ O ₂₇
Formula weight	432.38	1908.89	1310.97
Temperature/K	100	100	100
Crystal system	monoclinic	triclinic	monoclinic
Space group	<i>P2₁/n</i>	<i>P</i> -1	<i>P2₁/c</i>
<i>a</i> /Å	13.0286(4)	9.3062(3)	15.0689(6)
<i>b</i> /Å	6.9850(2)	20.1158(6)	22.3544(9)
<i>c</i> /Å	22.2051(6)	22.2589(7)	14.3047(6)
α /°	90	101.9120(10)	90
β /°	93.3610(10)	101.2140(10)	109.6750(10)
γ /°	90	98.7420(10)	90
Volume/Å ³	2017.29(10)	3918.4(2)	4537.3(3)
<i>Z</i>	4	2	4
ρ_{calc} /cm ³	1.424	1.618	1.919
μ /mm ⁻¹	0.999	0.894	1.495
F(000)	908	1940	2616
Crystal size/mm ³	0.17 × 0.08 × 0.06	0.25 × 0.09 × 0.02	0.40 × 0.24 × 0.05
Radiation	CuK α (λ = 1.54178)	MoK α (λ = 0.71073)	MoK α (λ = 0.71073)
2 Θ range for data collection/°	7.976 to 136.696	3.184 to 52.116	2.87 to 57.00
Index ranges	-15 ≤ <i>h</i> ≤ 15, -8 ≤ <i>k</i> ≤ 8, -26 ≤ <i>l</i> ≤ 26	-11 ≤ <i>h</i> ≤ 11, -24 ≤ <i>k</i> ≤ 24, -27 ≤ <i>l</i> ≤ 27	-20 ≤ <i>h</i> ≤ 20, -30 ≤ <i>k</i> ≤ 30, -19 ≤ <i>l</i> ≤ 19
Reflections collected	20803	68542	132473
Independent reflections	3693 [<i>R</i> _{int} = 0.0349, <i>R</i> _{sigma} = 0.0218]	15470 [<i>R</i> _{int} = 0.0719, <i>R</i> _{sigma} = 0.0683]	11504 [<i>R</i> _{int} = 0.0325, <i>R</i> _{sigma} = 0.0148]
Reflections Observed [<i>I</i> ≥ 2 σ (<i>I</i>)]	3353	10666	10328
Data/restraints/parameters	3693/30/338	15470/45/1126	11504/30/675
Goodness-of-fit on <i>F</i> ²	1.068	1.014	1.115
Final <i>R</i> indexes [<i>I</i> ≥ 2 σ (<i>I</i>)]	<i>R</i> ₁ = 0.0477, <i>wR</i> ₂ = 0.1359	<i>R</i> ₁ = 0.0504, <i>wR</i> ₂ = 0.1162	<i>R</i> ₁ = 0.0322, <i>wR</i> ₂ = 0.0807
Final <i>R</i> indexes [all data]	<i>R</i> ₁ = 0.0510, <i>wR</i> ₂ = 0.1408	<i>R</i> ₁ = 0.0884, <i>wR</i> ₂ = 0.1317	<i>R</i> ₁ = 0.0382, <i>wR</i> ₂ = 0.0852
Largest diff. peak/hole / e Å ⁻³	0.57/-0.31	1.24/-0.87	1.62/-1.02
CCDC Number	1812950	1812951	1812952

7. Gas Adsorption Data

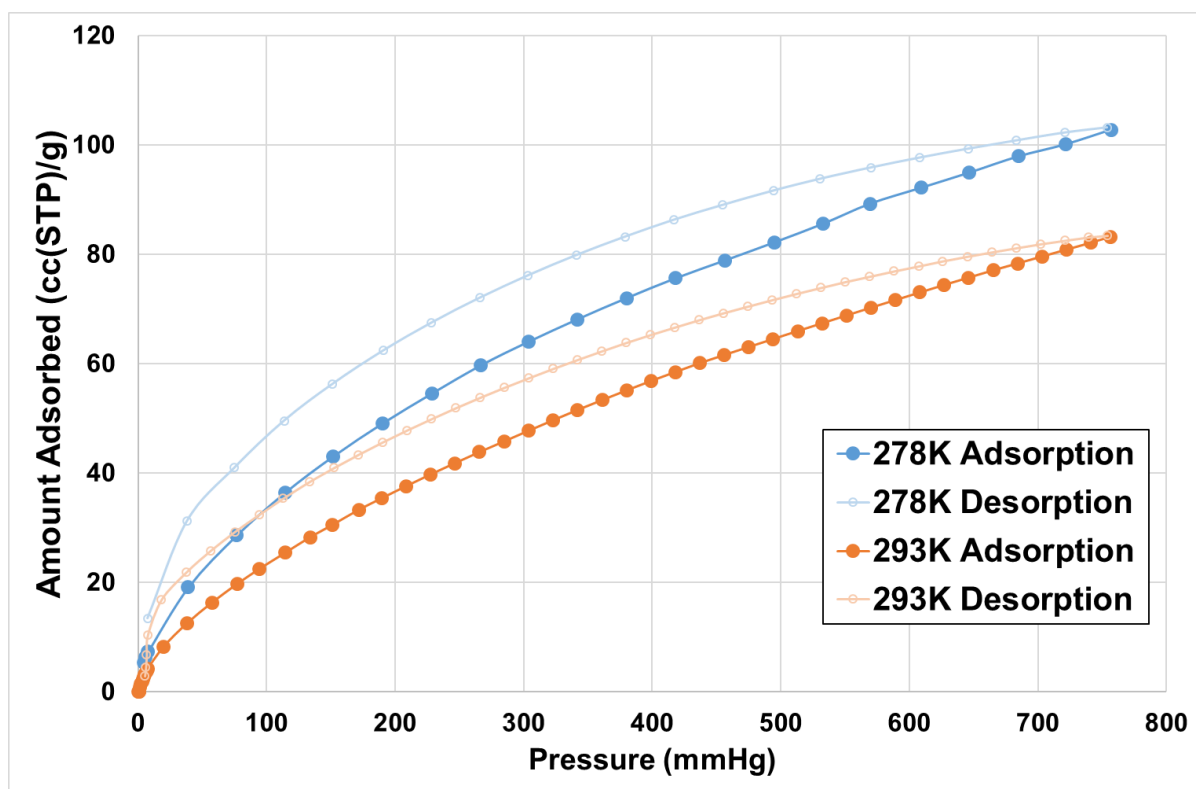


Figure S15 Adsorption and desorption branches for CO₂ uptake in complex 1

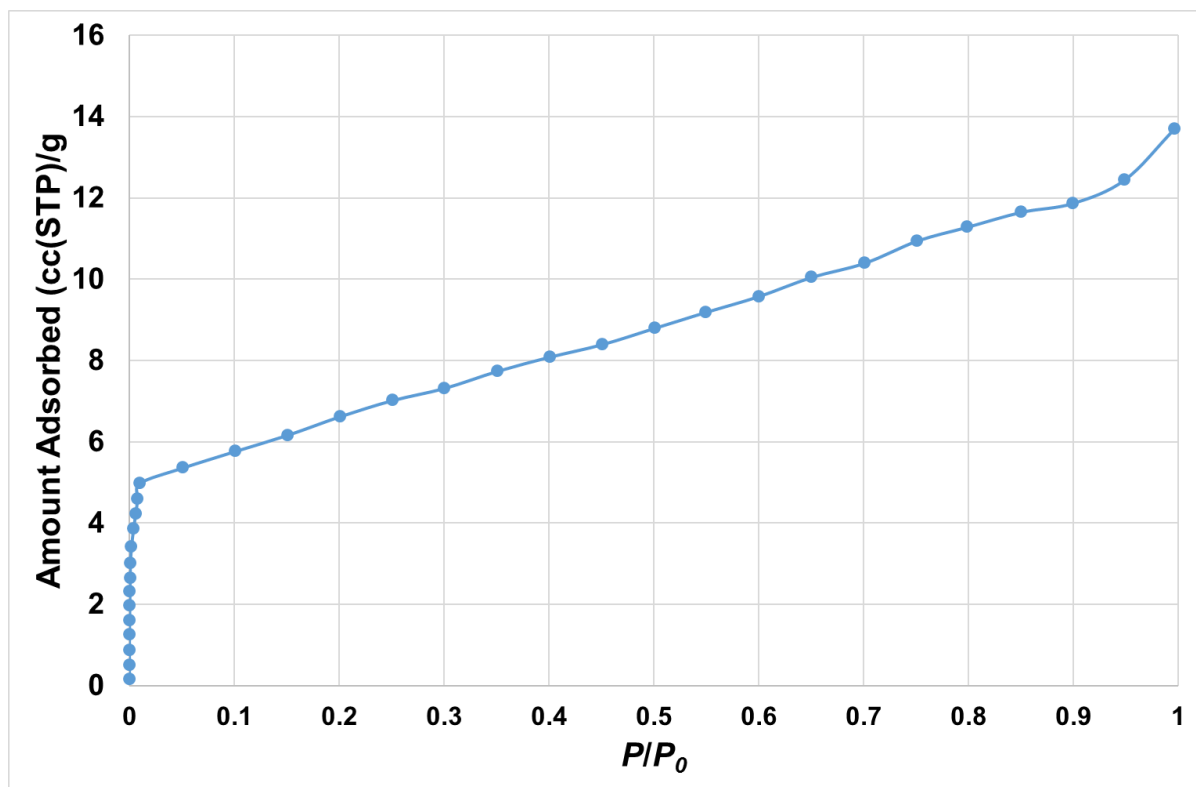


Figure S16 N₂ adsorption isotherm for complex 1 (77 K).

Isosteric Heat of Adsorption (CO₂) calculation

The isosteric heat of adsorption for CO₂ in complex **1** was estimated by least-squares fitting of a Virial-type adsorption equation modelling $\ln(P)$ as a function of adsorbed CO₂ quantity at 278 K and 293 K.^{S1} The model function was $\ln(P) = \ln(N) + (a_0 + a_1N + a_2N^2)/T + b$, (which was sequentially reduced from a 6-term series), giving the enthalpy of adsorption as $Q(N) = -R(a_0 + a_1N + a_2N^2)$. Virial coefficients and fitting parameters are given in Table S2 below, and the calculated Q_{ST} values are given in Figure S13.

Table S2 Fitting Parameters for Isosteric Heat of Adsorption Calculation

Temperatures (K)	278, 293
a ₀	-3318.7
a ₁	225.90
a ₂	-24.390
b	12.996
R ²	0.992
Datapoints Fitted	64

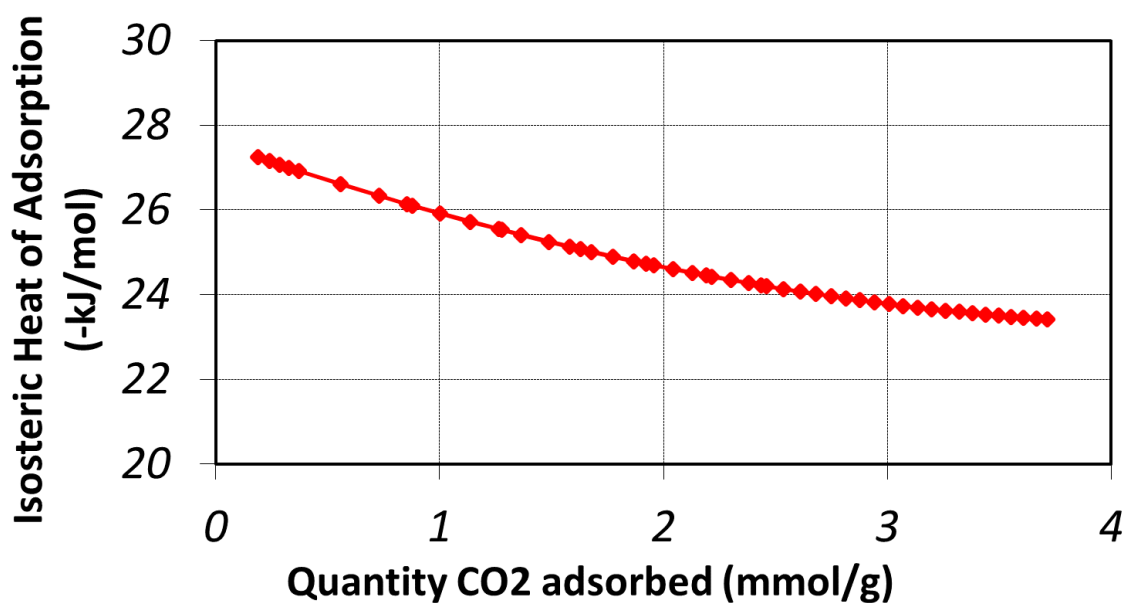


Figure S17 Estimated isosteric heat of adsorption for CO₂ in complex **1** as a function of adsorbed quantity.

Surface Area Calculations

Table S3 Parameters for BET surface area calculation (Compound 1, N₂, 77K):

Slope = 608.320
Intercept = 2.235e+00
Correlation coefficient, r = 0.998621
C constant= 273.134
Surface Area = 5.704 m ² /g

Table S4 Parameters for Dubinin-Radushkevich surface area calculations (Complex 1, CO₂, 278K)

Slope = -1.721e-01
Intercept = 2.271e-03
Correlation Coefficient = 0.9992
Average Half pore width = 7.068Å
Micropore volume = 0.069 cc/g
Micropore surface area = 206.930 m ² /g

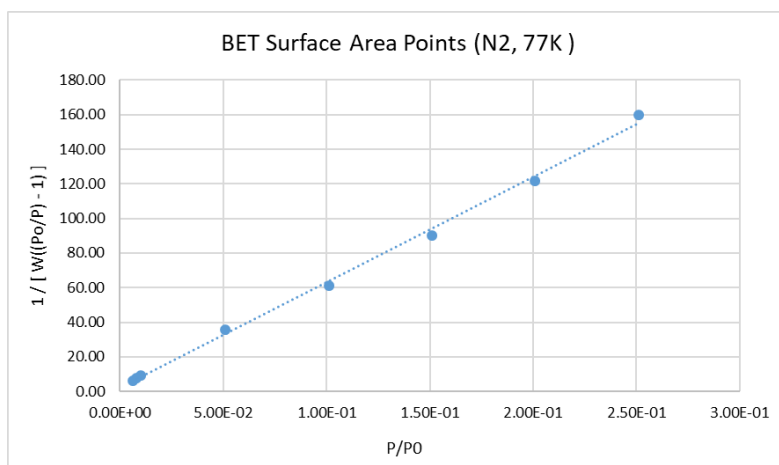


Figure S18 BET transformed isotherm plot for complex 1 (N₂, 77K)

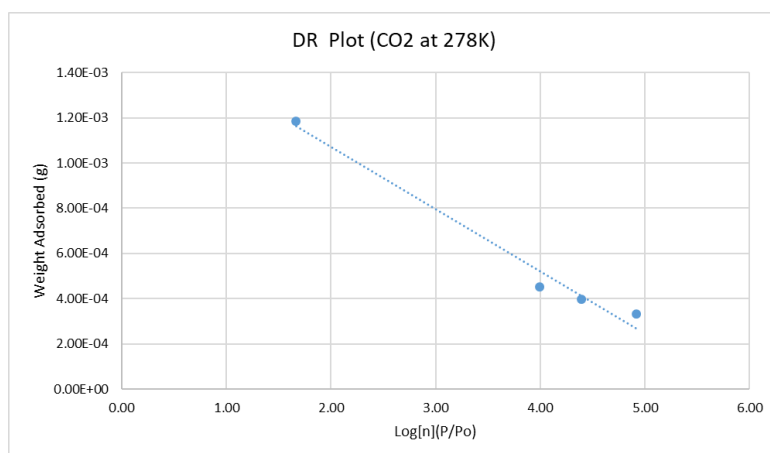


Figure S19 Dubinin-Radushkevich transformed isotherm plot for complex 1 (CO₂, 278K)

8. References

S1 L. Czepirski and J. Jagiello, *Chem. Eng. Sci.* 1989, **44**, 797-801; S. Tedds, A. Walton, D. P. Broom, and D. Book, *Faraday Discuss.* 2011, **151**, 75-94.